SCIENCE CHINA
Life Sciences

FROM CAS MEMBERS
• RESEARCH PAPER •

September 2016 Vol.59 No.9: 909–919
doi: 10.1007/s11427-016-5102-x

Enzymatic and chemical mapping of nucleosome distribution in purified micro- and macronuclei of the ciliated model organism, *Tetrahymena thermophila*

Xiao Chen[1], Shan Gao[1,2*], Yifan Liu[3], Yuanyuan Wang[1], Yurui Wang[1] & Weibo Song[1**]

[1]*Institute of Evolution & Marine Biodiversity, Ocean University of China, Qingdao 266003, China;*
[2]*Laboratory for Marine Biology and Biotechnology, Qingdao National Laboratory for Marine Science and Technology, Qingdao 266003, China;*
[3]*Department of Pathology, University of Michigan, Ann Arbor MI 48109, USA*

Received May 21, 2016; accepted June 12, 2016; published online August 23, 2016

Genomic distribution of the nucleosome, the basic unit of chromatin, contains important epigenetic information. To map nucleosome distribution in structurally and functionally differentiated micronucleus (MIC) and macronucleus (MAC) of the ciliate *Tetrahymena thermophila*, we have purified MIC and MAC and performed micrococcal nuclease (MNase) digestion as well as hydroxyl radical cleavage. Different factors that may affect MNase digestion were examined, to optimize mono-nucleosome production. Mono-nucleosome purity was further improved by ultracentrifugation in a sucrose gradient. As MNase concentration increased, nucleosomal DNA sizes in MIC and MAC converged on 147 bp, as expected for the nucleosome core particle. Both MNase digestion and hydroxyl radical cleavage consistently showed a nucleosome repeat length of ~200 bp in MAC of *Tetrahymena*, supporting ~50 bp of linker DNA. Our work has systematically tested methods currently available for mapping nucleosome distribution in *Tetrahymena*, and provided a solid foundation for future epigenetic studies in this ciliated model organism.

nucleosome, micrococcal nuclease digestion, hydroxyl radical cleavage, *Tetrahymena*, micronuclei, macronuclei

Citation: Chen, X., Gao, S., Liu, Y., Wang, Y., Wang, Y., and Song, W. (2016). Enzymatic and chemical mapping of nucleosome distribution in purified micro- and macronuclei of the ciliated model organism, *Tetrahymena thermophila*. Sci China Life Sci 59, 909−919. doi: 10.1007/s11427-016-5102-x

INTRODUCTION

Nucleosome is the basic repeating unit of chromatin in the nucleus of eukaryotic cells (Kornberg, 1974). The nucleosome core particle is comprised of 147 base pairs (bp) of nucleosomal DNA wrapped around a protein complex of two copies of each histone: H2A, H2B, H3 and H4 (Richmond and Davey, 2003; Sahasrabuddhe and Van Holde, 1974). Variable length of linker DNA exists between adjacent core particles (Spadafora et al., 1976). Nucleosomes regulate access to DNA, and controls gene expression, DNA replication and repair (Felsenfeld and Groudine, 2003; Sims et al., 2004; Thiriet and Hayes, 2005; Zentner and Henikoff, 2013).

Tetrahymena thermophila is a well-established unicellular eukaryotic model organism (Figure 1A–F) (Chen et al., 2015; Gao et al., 2016; Karrer, 1999). Like most ciliates, *Tetrahymena* exhibits nuclear dimorphism, containing one micronucleus (MIC) and one macronucleus (MAC) in the same cell compartment (Figure 1F) (Karrer, 2012). MIC is the germline nucleus that ensures the transmission of genetic information from generation to generation, while MAC is the somatic nucleus that provides "house-keeping" func-

*Corresponding author (email: shangao@ouc.edu.cn)
**Corresponding author (email: wsong@ouc.edu.cn)

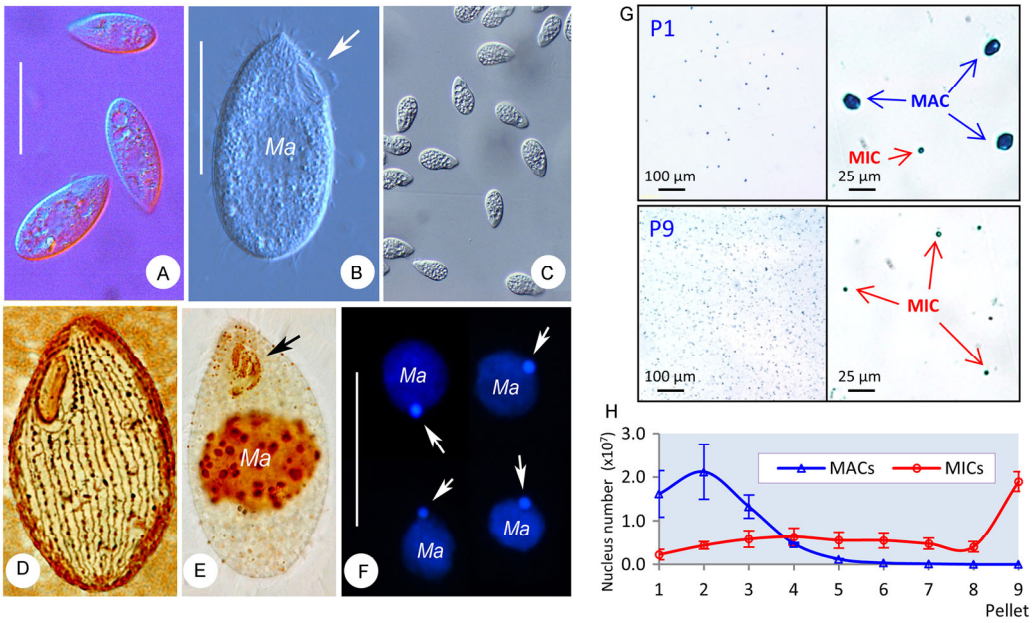

Figure 1 Purification of structurally and functionally differentiated MAC and MIC from *Tetrahymena thermophila*. A–F, Morphology of *Tetrahymena thermophila*. A–C, Phase-contrast imaging of live cells, arrow in (B) indicates the membranelles. D, Silverline system. E, Infraciliature on ventral side, arrow marks the oral apparatus. F, 4′,6-diamidino-2-phenylindole (DAPI) staining of MAC (Ma) and MIC (arrows). Scale bar=20 μm. G, Images of pellet 1 (600 g) and pellet 9 (5,000 g), after methylene blue staining. Pellet 1 shows many MACs as well as a few MICs; pellet 9 shows many MICs but no MAC. H, Number of MAC and MIC in each pellet, based on triplicate experiments.

tions leading directly to the cell phenotype (Chalker et al., 2013). MIC is diploid and transcriptionally silent except during sexual development (conjugation), whereas MAC is polyploidy (about 45×) and transcriptionally active during vegetative growth (Karrer, 2012). The zygotic nucleus, developed from parent MIC, differentiates into MAC during conjugation (Greider and Blackburn, 1985). There is dramatic DNA rearrangement during the differentiation of MIC and MAC, which is shaped by epigenetic information originated from MAC and represents an unambiguous manifestation of trans-generational transmission of epigenetic information (Gao and Liu, 2012; Mochizuki and Gorovsky, 2004; Schoeberl and Mochizuki, 2011).

Chromatin fragmentation is the first step for mapping nucleosome distribution, for which micrococcal nuclease (MNase) digestion is generally used. MNase is an endonuclease/exonuclease that preferentially cut linker DNA, often resulting in a DNA ladder corresponding to mono-nucleosomes and oligo-nucleosomes (Cui and Zhao, 2012; Noll and Kornberg, 1977). MNase digestion, followed by microarray or deep-sequencing, has been widely adapted in the studies of genome-wide nucleosome distribution in a wide-variety of organisms (Barski et al., 2007; Beh et al., 2015; Fraser et al., 2009; Kaplan et al., 2009; Mavrich et al., 2008; Ozsolak et al., 2007; Schones et al., 2008; Valouev et al., 2008).

Hydroxyl radical cleavage was first developed to map distribution of *in vitro* reconstituted nucleosomes (Flaus et al., 1996). It has been adapted for mapping of *in vivo* nucleosome distribution in *Saccharomyces cerevisiae* at base-pair resolution (Brogaard et al., 2012a). Briefly, after serine 47 of histone H4 protein is mutated to a cysteine (H4 S47C), nucleosomal DNA can be precisely cleaved at sites adjacent to the nucleosomal dyad by hydroxyl radicals generated by hydrogen peroxide and chelated Cu^{+} (Flaus et al., 1996). Its precise cleavage and lack of sequence bias provide a valuable alternative to MNase digestion for high resolution mapping of nucleosome distribution (Brogaard et al., 2012a).

Here we studied enzymatic and chemical cleavage of *Tetrahymena* MAC and MIC chromatin. Different factors affecting MNase digestion were examined to optimize mono-nucleosome production. Mono-nucleosomal DNA was further purified using agarose gel electrophoresis or sucrose gradient ultracentrifugation. Essentially the same nucleosome repeat length was produced by hydroxyl radical cleavage as MNase digestion of the MAC chromatin, validating the applicability of both approaches in studying nucleosome distribution in *Tetrahymena*.

RESULTS AND DISCUSSION

Preparation of high purity MAC and MIC samples by differential centrifugation

In *Tetrahymena*, the polyploid MAC and diploid MIC are substantially different in size (~10 and 1 μm in diameter, respectively), allowing separation by differential centrifugation with gradually increasing g values (Figure 1G and H;

Table S1 in Supporting Information). Specifically, MACs can be purified at low g values (Figure 1G). Most MACs were collected in the first five pellets (at 600, 800, 1,000, 1,200, and 1,400 g) (Figure 1H). MIC accounted for about 10%–20% of total nuclei by number in the first two pellets (~1% by DNA content) (Table S1 in Supporting Information). The MIC/MAC ratio increased with g values. In the last pellet (pellet 9), ~20% MIC were recovered at 5,000 g (Figure 1H), at >99.9% purity by number (~99% by DNA content) (Figure 1G). For nuclear preparation to achieve high recovery and high purity, it is important for cell density to not exceed 2.5×10^5 cells mL^{-1} (mid-log phase). As previously reported, stationary phase culture required additional amounts of 1-octanol or extra blending to prepare nuclei (Gorovsky et al., 1975). Moreover, MIC is more tightly attached to MAC in stationary-phased cells, reducing the purity of MAC and even causing failure in MIC purification.

General approaches for mapping nucleosome distribution

With purified MAC and MIC, we performed enzymatic and chemical cleavage of chromatin to map their nucleosome distribution, as illustrated in a flowchart (Figure 2). Micrococcal nuclease (MNase) was used for partial digestion of chromatin, as previously established in *Tetrahymena* as well as other systems (Gorovsky et al., 1978). The digestion condition was optimized to generate the mono-nucleosome from both MAC (Figure 3) and MIC (Figure 4). Mono-nucleosomal DNA was further enriched by agarose gel purification. Alternatively, mono-nucleosomes were enriched by ultra-centrifugation in a sucrose gradient (Figure 5). Paired-end Illumina sequencing was subsequently performed on the recovered mono-nucleosome sized DNA fragments. Analysis of sequencing results revealed arrays of strongly positioned nucleosomes with ~200 bp nucleosome repeat length (NRL) present in MAC, while this periodic nucleosome distribution pattern was dramatically reduced in MIC (Figures 3 and 4). By comparing the MAC and MIC results, we dissected relative contributions of *cis*-determinants and *trans*-determinants to nucleosome distribution (manuscript under review). *Tetrahymena* is one of the few model systems in which histone mutagenesis can be readily performed (Liu et al., 2004), allowing complete replacement of endogenous histones with mutated ones needed for Cu^+ chelation, hydroxyl radical production, and subsequent cleavage of nucleosomal DNA around the dyad (Brogaard et al., 2012a). DNA fragments corresponding to ~200 bp NRL was generated by chemical cleavage, establishing it as a valid alternative for mapping nucleosome distribution in *Tetrahymena* (Figure 6).

Optimization of MNase digestion for MAC

In order to optimize the MNase digestion condition for MAC, we tested several factors (Figure 3 and Table 1): (i) MNase concentration, (ii) 1-octanol concentration, (iii) de-

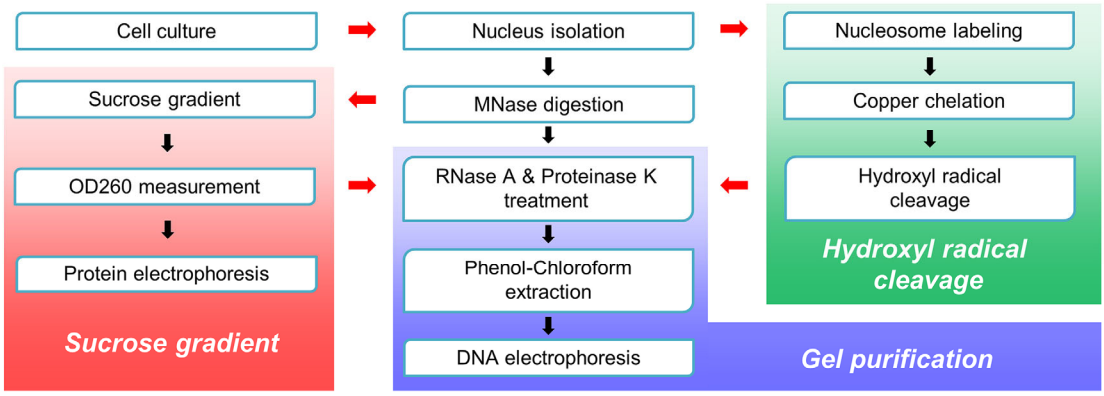

Figure 2 A workflow for enzymatic and chemical mapping of nucleosome distribution in *Tetrahymena*. These include MAC/MIC purification, MNase digestion or hydroxyl radical cleavage of chromatin, and mono-nucleosome sized DNA purification (by sucrose gradient ultracentrifugation or agarose gel purification).

Table 1 Different factors that may affect the MNase digestion pattern in MAC.

Factors	Options	Description
Centrifugal force	1,500 g	sufficient to collect most MACs according to Figure 1H
MNase concentration	50/100/200 Kunitz units mL^{-1}	heavy digestion promoting the yield of mono-nucleosomes
1-octanol	0.32%/0.63%	no significant influence
Nonidet P-40 and β-mercaptoethanol	+/–	no significant influence
T150 buffer with Triton X-100 and protease inhibitor	+/–	will promoting yield if exists
RNase A treatment	+/–	no significant influence

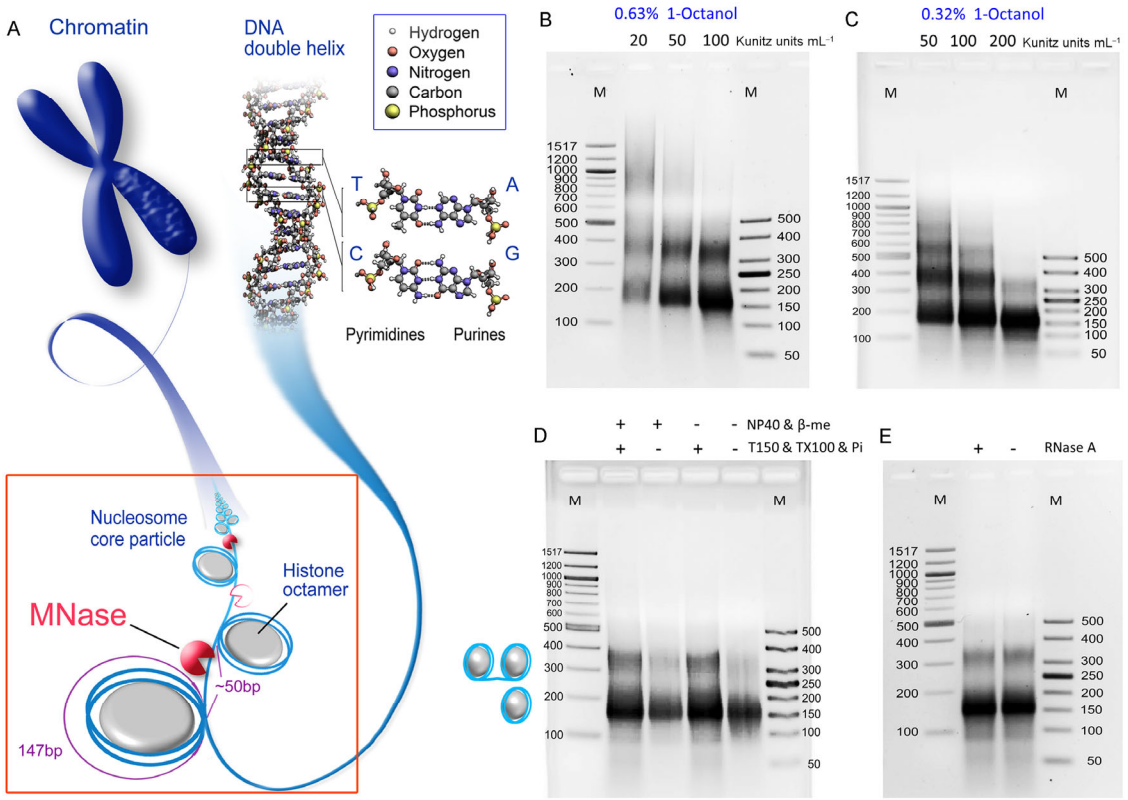

Figure 3 Different factors affecting MNase digestion of MAC. A, Hierarchical organization of chromatin. Mono-nucleosomes and oligo-nucleosomes can be generated by limited MNase digestion. Mono-nucleosomes may contain only DNA within a nucleosome core particle (147 bp), while di-nucleosomes, generated by insufficient MNase digestion (indicated by the hollow pattern), contain DNA within two nucleosome core particle as well as the linker DNA between them (~350 bp). B, Digestion pattern with 0.63% 1-octanol and 20, 50, 100 Kunitz units mL^{-1} MNase. C, Digestion pattern with 0.32% 1-octanol and 50, 100, 200 Kunitz units mL^{-1} MNase. D, Effect of nonidet P-40 and β-mercaptoethanol (+, –), and T150 buffer with Triton X-100 and protease inhibitor (+,–), on chromatin fragmentation and nucleosome recovery. E, RNase A treatment (+, –).

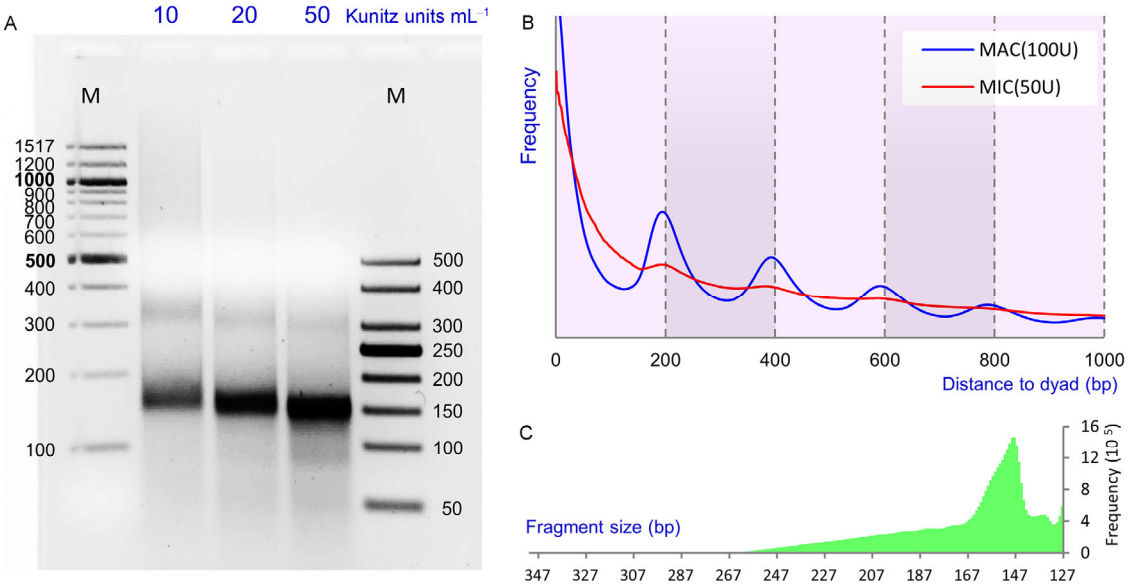

Figure 4 MIC MNase digestion and mono-nucleosomal DNA sequencing (MNase-Seq). A, MIC MNase digestion pattern with 0.32% 1-octanol and 10, 20, 50 Kunitz units mL^{-1} MNase. B, Phasogram of mono-nucleosomal DNA in MIC and MAC. The MIC sample was digested in 50 Kunitz units mL^{-1} MNase, while the MAC sample was digested in 100 Kunitz units mL^{-1} MNase. C, Fragment size distribution of MIC mono-nucleosomal DNA produced by MNase-Seq with 50 Kunitz mL^{-1} MNase.

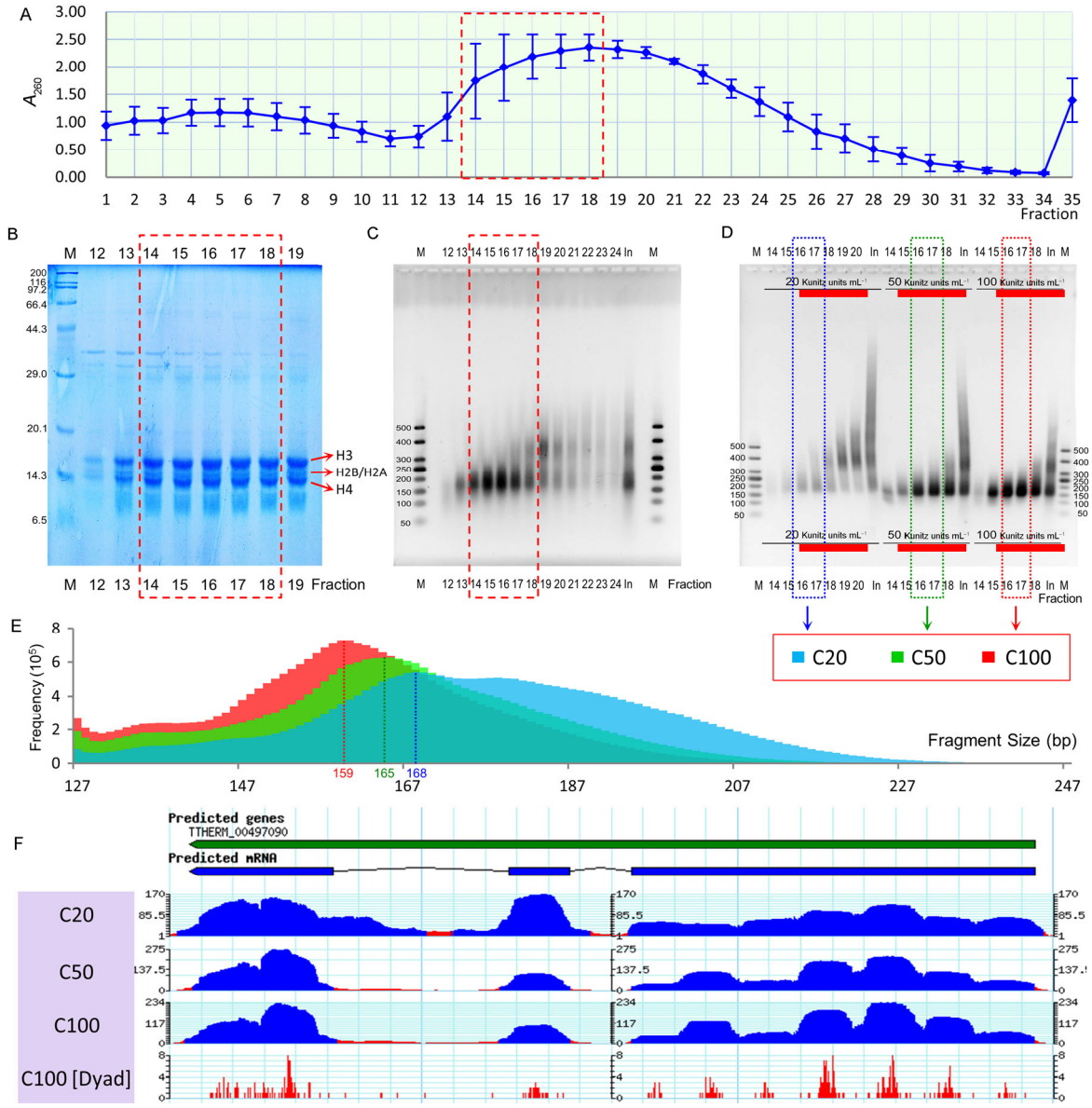

Figure 5 Mono-nucleosome purification by ultracentrifugation in a sucrose gradient. A, A_{260} values of each fraction after sucrose gradient ultracentrifugation (from top to bottom) identified those containing nucleosomes. The MAC sample was digested with 50 Kunitz units mL^{-1} MNase. B, Coomassie brilliant blue staining confirmed the presence of only core histones in mono-nucleosome fractions. C, 2% of each fraction was analyzed by agarose gel electrophoresis. Input was labeled as "In". D, Fractions containing mono-nucleosome sized DNA after MNase digestion under different concentrations were collected and sequenced. Input was labeled as "In". E, Fragment size distribution of MAC mono-nucleosomal DNA produced by MNase-Seq with different MNase digestion concentration. C20: 20 Kunitz units mL^{-1} (CU428), peaking at 168 bp; C50: 50 Kunitz units mL^{-1} (CU428), peaking at 165 bp; C100: 100 Kunitz units mL^{-1} (CU428), peaking at 159 bp. F, Mapping results of mono-nucleosomal DNA produced by MNase-Seq with different MNase digestion concentration shown in Gbrowse.

tergents (nonidet P-40 and Triton X-100), (iv) protease inhibitors, and (v) RNase A treatment. This allows us to maximize the mono-nucleosome yield and purity from MAC samples.

MNase has a strong preference to cleave linker DNA (Figure 3A), releasing mono-nucleosomes and oligo-nucleosomes under proper digestion conditions. We performed digestion with varying MNase concentration at 25°C for 15 min (Figure 3B and C). At 20 or 50 Kunitz units mL^{-1} MNase, agarose gel electrophoresis showed DNA ladders corresponding to mono-nucleosomes and oligo-nucleosomes. At 100 Kunitz units mL^{-1} MNase, the bulk of DNA was from mono-nucleosomes, with only a small fraction from di-nucleosomes. 200 Kunitz units mL^{-1} MNase generated mostly mono-nucleosome sized fragments, but there was also substantial amount of sub-

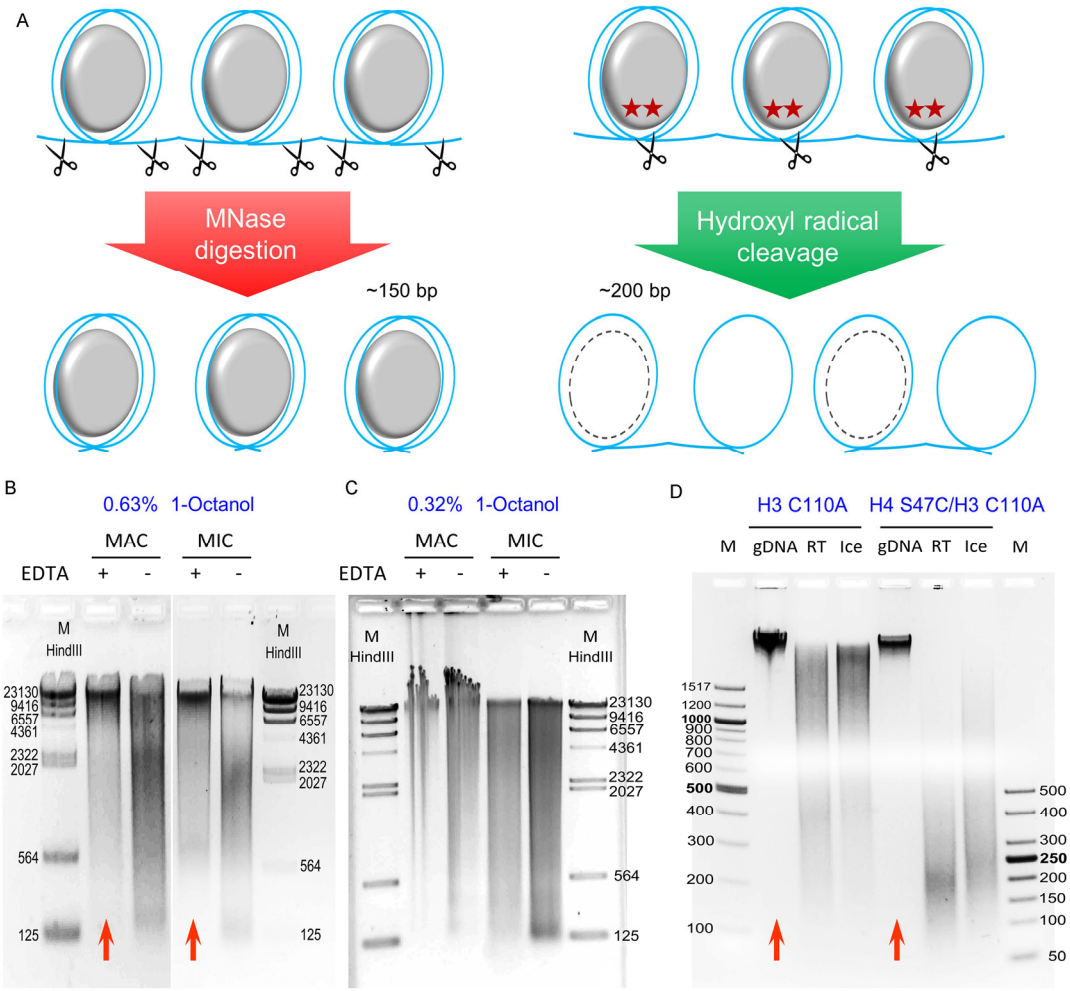

Figure 6 Hydroxyl radical cleavage of *Tetrahymena* chromatin. A, Comparison between enzymatic and chemical mapping of nucleosome distribution. Left: MNase digests linker DNA between nucleosomes, and leaves mono-nucleosomes with ~150 bp DNA; right: chelated copper I (red asterisk) catalyzes local production of hydroxyl radicals, which cleave nucleosomal DNA precisely at sites adjacent to the dyads, and generate nucleosome repeat length DNA, at ~200 bp. B, gDNA of MAC and MIC purified with 0.63% 1-octanol and 20 mmol L^{-1} EDTA (+, –). Red arrows indicated intact gDNA. C, gDNA of MAC and MIC purified with 0.32% 1-octanol and 20 mmol L^{-1} EDTA (+, –). D, Hydroxyl radical cleavage of MAC chromatin from H3 C110A (left, negative control) and H4 S47C/H3 C110A cells (right). Note the limited fragmentation in H3 C110A sample, and the extensive fragmentation as well as the ~200 bp band in H4 S47C/H3 C110A sample. Red arrows indicated intact gDNA.

nucleosome fragments, indicative of over-digestion (Figure 3C). We therefore decided to use 100 Kunitz units mL^{-1} MNase for subsequent digestion of *Tetrahymena* MAC samples.

1-octanol, an amphiphilic molecule, is used in *Tetrahymena* nuclear preparation to form a "skin", sequestering cell debris from nuclei (Gorovsky, 1970). It also stabilizes nuclear membrane, which may affect chromatin solubilization and extraction. We performed MAC purification with reduced amount of 1-octanol (0.32%), compared with a preparation with the original amount (0.63%) recommended by Gorovsky et al. (Gorovsky et al., 1975). Reducing 1-octanol concentration did not lower the yield of mono-nucleosomes, and only slightly affected the laddering pattern of MNase digestion at different MNase concentrations (Figure 3B and C). We therefore kept 1-octanol at 0.63% for subsequent MAC purification.

Nonidet P-40 (NP-40) is a mild detergent often used for membrane permeabilization, while preserving nuclear integrity (Liu et al., 2014). 2-Mercaptoethanol (2-ME) is a reducing agent often included in enzymatic reactions to prevent oxidation of the sulfhydryl group and hence maintain enzymatic activities (Verduyn et al., 1985). As shown in Figure 3D, the addition of NP-40 (1%) and 2-ME (10 mmol L^{-1}) during MNase digestion only slightly affected the laddering pattern of MNase digestion, compared with the control group. Nonetheless, we decided to keep NP-40 and 2-ME in subsequent MNase digestion, as they are routinely included in the standard protocol.

MNase digestion is performed with low salt. After MNase digestion, increasing salt concentration and adding detergent may promote chromatin solubilization and extrac-

tion. Here we tested an extraction buffer containing 150 mmol L^{-1} NaCl, 0.1% Triton X-100, and protease inhibitor cocktail. This buffer also provides a more stringent environment for protein-protein interactions, which will increase the antibody binding specificity and signal-to-noise ratio in downstream experiments like native chromatin immunoprecipitation (N-ChIP) (Nelson et al., 2006). Our result showed that the extraction buffer produced a dramatic increase in the yield of mono-nucleosomes, and even more so, di-nucleosomes (Figure 3D). Interestingly, mono-nucleosomes represented a higher proportion of total products from samples not treated with the extraction buffer, possibly attributed to reduced permeability of nuclear membranes as well as chromatin solubilization. In subsequent experiments, the extraction buffer was always used after MNase digestion to maximize the yield.

Although MNase can degrade both DNA and RNA (Cuatrecasas et al., 1967), *Tetrahymena* MAC (Karrer, 2012), with high transcription activities, numerous nucleoli, and abundant rRNA, may present a particular challenge. To address this concern, RNase A treatment was carried out after MNase digestion (Figure 3E). The DNA ladders of MNase digestion were exactly the same with or without subsequent RNase A treatment. This indicates that RNA is completely degraded by MNase digestion and an extra step for RNase A treatment is not necessary.

Optimization of MNase digestion for MIC

MNase digestion of MIC samples did not generate an obvious laddering pattern as MAC (Figure 4A). There was only one predominant band corresponding to mono-nucleosomes, even under 10 Kunitz units mL^{-1} MNase; while 100–200 Kunitz units mL^{-1} MNase was needed to generate predominantly mono-nucleosomes for MAC. This result may be caused by several factors: (i) reduced substrate concentration: as input for MNase digestion, the DNA content for the MIC sample was much lower than the MAC sample (~5%); (ii) increased and more uniform accessibility to MNase: MIC is much smaller than MAC in size (~1 and 10 μm in diameter, respectively), and its content may be more readily accessed by diffusion; (iii) variable linker DNA length: the laddering pattern of MAC is the result of uniform linker DNA length therein, while its missing in MIC may reflect highly variable linker DNA length. Further experimentation is needed to sort out these possibilities.

As MNase concentration increased from 10, 20 Kunitz units mL^{-1} to 50 Kunitz units mL^{-1}, the smear corresponding to large DNA fragments diminished, while the clear band corresponding to the mono-nucleosome increased in intensity (Figure 4A). With increasing MNase concentration, there was also a progressive decrease of mono-nucleosomal DNA length, gradually approaching 147 bp (corresponding to the size of the nucleosome core particle). The mono-nucleosomal DNA generated by 50 Kunitz units mL^{-1} MNase was paired-end sequenced and mapped to the MIC reference genome (Table 2). Phasogram analysis showed that nucleosome periodicity in MIC was much weaker than that in MAC (at ~200 bp), supporting that nucleosome distribution was more disorganized in MIC than MAC (Figure 4B). Analysis of sequencing result also revealed a peak at 147 bp in the fragment size distribution (Figure 4C), consistent with the agarose gel electrophoresis result (Figure 4A).

Purification of mono-nucleosomes by utracentrifugation in a sucrose gradient

Mono-nucleosomes can be effectively separated from oligo-nucleosomes by ultra-centrifugation in a sucrose gradient (O'Neill and Turner, 2003). We adapted the procedure to fraction the MAC MNase digestion products, using a step gradient that is easier to prepare (5%, 10%, 15%, 20%, 25% sucrose). Nucleosome-containing fractions were revealed by elevated A_{260} values (indicative of DNA concentration) (Figure 5A; Table S2 in Supporting Information). These fractions were further analyzed for their protein content by SDS-PAGE (Figure 5B), and DNA content by agarose gel electrophoresis (Figure 5C). Mono-nucleosome were enriched in fractions 14–18, in which Coomassie brilliant blue staining of protein gel showed predominantly core histones, while the DNA gel showed predominantly 150–200 bp fragments (Figure 5B and C). Using this method, we enriched mono-nucleosome fractions from MAC samples digested with different MNase concentrations (20, 50, 100 Kunitz units mL^{-1}) (fractions 16 and 17, Figure 5D and Table 2). Analysis of sequencing results revealed decreasing fragment sizes with increasing MNase concentrations (Figure 5E). The result was consistent with increased mobility observed in agarose gel electrophoresis (Figure 3B and C), and indicative of progressive removal of the linker DNA by MNase. A representative snapshot in Gbrowse illustrated the distribution of the mono-nucleosomes produced by different MNase digestion concentration (20, 50, 100 Kunitz units mL^{-1}) after mapping pair-end reads to the MAC genome (Figure 5F), revealing progressive depletion of the

Table 2 Sequencing information of MAC/MIC mono-nucleosomal DNA samples after MNase digestion.

Sample	MNase digestion (Kunitz units mL^{-1})	Strain	Purification	Input	Mapped reads	Unique mapped reads	non-MDS unique mapped reads	Percentage of non-MDS reads
MIC	50	CU428	Gel purification	131,754,966	102,186,811	99,659,285	29,611,205	29.71%
MAC1	20	CU428	Sucrose gradient	56,868,076	54,422,059	52,264,892	382,320	0.67%
MAC2	50	CU428	Sucrose gradient	52,076,454	49,336,271	47,118,038	308,826	0.59%
MAC3	100	CU428	Sucrose gradient	55,796,824	52,607,335	50,248,546	347,728	0.62%

linker DNA coverage. We conclude that sucrose gradient ultracentrifugation can yield high-quality mono-nucleosomes, providing ideal inputs for ChIP studies.

Chemical mapping of nucleosome distribution

Lastly, hydroxyl radical cleavage was applied in *Tetrahymena* to study nucleosome distribution. While MNase digestion progressively removes the linker DNA, leaving mono-nucleosomes as the key product, hydroxyl radical cleavage occurs at two symmetric sites 6 bp away from the nucleosome dyad, allowing direct measurement of the exact position of a nucleosome and nucleosome repeat length (NRL) at base-pair resolution (Figure 6A). Using an established histone mutagenesis procedure (Liu et al., 2004), H4 S47C mutation was introduced into *Tetrahymena*, allowing a chelated Cu^{+} to be positioned near the nucleosome dyad, as well as localized production of hydroxyl radical and cleavage of nucleosomal DNA (Brogaard et al., 2012a; Flaus et al., 1996). Similarly, H3 C110A mutation was introduced to limit spurious reactions. As a negative control for the H4 S47C/H3 C110A strain, a *Tetrahymena* strain containing the H3 C110A mutation only was also generated and tested for hydroxyl radical cleavage (Figure 6D).

We first tested the genomic DNA integrity in samples prepared under different conditions (Figure 6B and C). Our result showed that using 0.63% 1-octanol during nuclear preparation and adding 20 mmol L^{-1} EDTA during DNA purification prevented DNA degradation in both MAC and MIC samples, compared with 0.32% 1-octanol and EDTA-free conditions. Adapting the reported procedure for hydroxyl radical cleavage for mapping MAC nucleosome distribution (Brogaard et al., 2012a, b; Moyle-Heyrman et al., 2013), we showed that DNA from the H4 S47C/H3 C110A strain were extensively fragmented, with a band at ~200 bp emerging from the background smear, while DNA from the H3 C110A strain stayed largely intact (Figure 6D). Hydroxyl radical cleavage was temperature sensitive, proceeding at a much faster rate at room temperature than on ice (Figure 6D). Our result establishes hydroxyl radical cleavage as a valid alternative for mapping nucleosome distribution in *Tetrahymena*, and confirms MAC nucleosome repeat length, at ~200 bp, as measured by MNase digestion. Further experimentation is needed for optimization of the hydroxyl radical cleavage procedure in *Tetrahymena*, particularly to increase the signal-to-noise ratio. Unlike MNase digestion, hydroxyl radical cleavage does not show significant AT bias, providing a high-resolution alternative for mapping high AT% genomic DNA, including inter-genic and intronic regions in MAC, and germline-specific sequences in MIC.

CONCLUSIONS

Purification of structurally and functionally differentiated MAC and MIC from the ciliated model organism *Tetrahymena thermophila* provides a unique opportunity for chromatin biology and epigenetic studies. Nucleosome distribution in MAC and MIC is mapped by enzymatic and chemical cleavage of chromatin. Various factors affecting MNase digestion are examined to optimize mono-nucleosome production. Ultra-centrifugation in a sucrose gradient allows further purification of mono-nucleosomes. Illumina sequencing of nucleosomal DNA generates genome-wide nucleosome distribution data, allowing us to dissect relative contributions of *cis*- and *trans*-determinants by comparing MAC and MIC chromatin. As an alternative to MNase digestion, hydroxyl radical cleavage can potentially map nucleosome distribution at base-pair resolution and with little sequence bias. Adapting the yeast protocol to *Tetrahymena*, chromatin fragmentation is observed in the H4 S47C/H3 C110A strain, but not in the H3 C110A strain which is the negative control in the hydroxyl radical cleavage. Furthermore, the same nucleosome repeat length in MAC, at ~200 bp, is revealed by MNase digestion and hydroxyl radical cleavage, corroborating the validity of these two independent approaches. By delineating the nucleosome distribution patterns in MAC and MIC, our study lays the groundwork for genome-wide mapping of epigenetic marks, many of which are conserved from *Tetrahymena* to mammals. Our work also sets the stage for characterizing the transition state(s) during MIC to MAC differentiation, shedding light on mechanisms reshaping the chromatin landscape upon transcription activation and repression.

MATERIALS AND METHODS

Cell culture

Tetrahymena thermophila wild-type strain CU428 was grown in 1×SPP medium at 30°C with shaking at 120 rpm to mid-log phase at ~ 2×10^5 cells mL^{-1} (Cassidy-Hanley et al., 1997; Ning et al., 2015).

Purification of MICs and MNase digestion of MIC samples

Nuclear preparation methods were modified from the published protocols (Gorovsky et al., 1975; Papazyan et al., 2014; Sweet and Allis, 2005). Mid-log phase cells were collected by centrifugation (350×*g*, 5 min), and resuspended in Medium A. Cells were ruptured in a blender (Waring 7011HS, USA) at the "High" setting for 60 s with 0.63% or 0.32% [v/v] 1-octanol (Acros Organics, USA), 1 mmol L^{-1} phenylmethanesulfonyl fluoride (PMSF) and 5 mmol L^{-1} ethylene diamine tetraacetic acid (EDTA). The released MACs were removed by differential centrifugation with increasing g values (600 to 2,000×*g*, with 200×*g* increments, 5 min) (pellets 1–8) (Thermo Scientific Sorvall LYNX 6000 centrifuge, USA; rotor: BIOFlex HC). Nuclear pellets were stained with methylene blue and monitored by microscopy. Afterwards, MICs were collected by centrifu-

gation at 5,000×*g* for 10 min. As long as the same number of cells (1×10^8) was used for each preparation, MAC and MIC can be recovered reproducibly. MIC samples (pellet 9) containing less than 0.1% MACs contamination were used in following procedures.

Subsequently, 10/20/50 Kunitz units mL^{-1} of micrococcal nuclease (MNase, NEB, USA) were added to MIC samples (2×10^7) in MNase digestion buffer (5 mmol L^{-1} Tris-HCl pH 8, 0.5 mmol L^{-1} $CaCl_2$, 0.1 mg mL^{-1} albumin from bovine serum (BSA)) with 1% nonidet P-40 (Sigma, USA) and 10 mmol L^{-1} 2-mercaptoethanol, and incubated at 25°C for 15 min. Mono-nucleosomal DNA was purified by agarose gel electrophoresis.

Purification of MACs and MNase digestion of MAC samples

After MACs were released in blender as described above, they were collected by centrifugation at 1,500×*g* for 10 min. Nuclear pellets were stained with methylene blue and monitored by microscopy. Subsequently, 20/50/100/200 Kunitz units mL^{-1} of micrococcal nuclease (MNase, NEB) were added to MAC samples (5×10^7) in MNase digestion buffer with 1% nonidet P-40 and 10 mmol L^{-1} 2-Mercaptoethanol, and incubated at 25°C for 15 min. Mono-nucleosomal DNA was purified by agarose gel electrophoresis or sucrose gradient ultracentrifugation.

Mono-nucleosomal DNA purification by agarose gel electrophoresis

The MNase digestion reaction was stopped by adding 10 mmol L^{-1} Ethylenebis (oxyethylenenitrilo) tetraacetic acid (EGTA), 1 mmol L^{-1} EDTA and 1% [v/v] sodium dodecyl sulfate (SDS). DNA was recovered by phenol-chloroform purification after RNase A (100 μg mL^{-1}) and Proteinase K (1 mg mL^{-1}) treatment in T150 buffer (30 mmol L^{-1} Tris-HCl pH 7.5 containing 150 mmol L^{-1} NaCl) (O'Neill and Turner, 2003), adding 0.1% Triton X-100 and EDTA-free protease inhibitor (complete cocktail, Roche, Switzerland). Mono-nucleosome sized DNA was sized selected by agarose gel electrophoresis, recovered by Zymoclean gel DNA recovery kit (Zymo Research, USA), and processed for Illumina paired-end sequencing.

Mono-nucleosomal DNA purification by sucrose gradient ultracentrifugation

0.1% [v/v] Triton X-100 was added for permeabilization after MNase digestion. 5% of each sample was kept as Input. Mono-nucleosome was collected by ultracentrifugation at 103,000×g, 4°C for 17 h in the sucrose gradient buffer (5/10/15/20/25% sucrose, 10 mmol L^{-1} Tris-HCl pH 8.0, 0.1 mmol L^{-1} EDTA, 0.1 mol L^{-1} NaCl, 5 mmol L^{-1} Na Butyrate) (O'Neill and Turner, 2003). Supernatant was taken as fractions (200 μL per fraction) layer by layer from top to bottom. Light absorption values A_{260} of each fraction in UV compatible 96-well plates were measured using a microplate reader (Tecan Infinite F200, Switzerland). The presence of histones was validated by Coomassie brilliant blue staining after SDS-PAGE. DNA was recovered by phenol-chloroform extraction and ethanol precipitation. 5% of each sample was analyzed by agarose gel electrophoresis, and fractions containing mono-nucleosome sized DNA were processed for Illumina paired-end sequencing.

Illumina sequencing and data processing

Illumina libraries were prepared from mono-nucleosomal DNA according to manufacturer's instructions, and paired-end sequencing (125 bp reads length) was performed using an Illumina HiSeq2500 sequencer. MNase-Seq reads of each sample were initially mapped to the genome assembly of *T. thermophila* (SB210), using Bowtie 2 (Langmead and Salzberg, 2012) allowing 2 edit distances including mismatch and indel. For the MAC MNase-Seq data, the reads were mapped to the latest MAC genome assembly in *Tetrahymena* genome database (TGD) (http://ciliate.org) (Eisen et al., 2007; Stover et al., 2012); for the MIC MNase-Seq data, the reads were mapped to the *T. thermophila* MIC genome assembly from the *Tetrahymena* Comparative Sequencing Project (http://www.roadinstitute.org/annotation/genome/Tetrahymena). Unique mapped reads were extracted, and only one of any potential PCR duplicates (fragments, defined by a pair of properly mapped reads, with the same location in genome) were kept (Gao et al., 2013). Only mono-nucleosome sized fragments (120 to 260 bp) were analyzed. The mapped reads were visualized using Gbrowse2 (Stein, 2013). Periodicity in the MNase-Seq data of both MAC and MIC samples was identified by phasogram (Valouev et al., 2011), using all fragment centers across the genome.

Hydroxyl radical cleavage

Hydroxyl radical cleavage was performed according to a protocol modified from published yeast studies (Brogaard et al., 2012a, b; Moyle-Heyrman et al., 2013). *T. thermophila* wild-type strain CU428 was genetically engineered to contain a cysteine at position 47 in histone H4 and an alanine at position 110 in histone H3 (H4 S47C/H3 C110A). Cells grown to mid-log phase (~ 2×10^5 cells mL^{-1}) were collected, and MAC were purified, permeabilized and labelled with N-(1,10 phenanthroline-5-yl) iodoacetamide (rotation at 4°C overnight, in the dark). The label, covalently bound to cysteine, allowed for copper chelation. Copper chloride, mercaptoproprionic acid and hydrogen peroxide were added sequentially, creating hydroxyl radicals that would cleave the nucleosomal DNA at sites flanking the dyad. After the mapping reaction, the genomic DNA was purified from MAC samples and resolved by agarose electrophoresis.

Compliance and ethics *The author(s) declare that they have no conflict of interest.*

Acknowledgements *We are grateful to Dr. Sean D. Taverna, Department of Biochemistry and Molecular Genetics, University of Virginia Health System for sharing a protocol for MIC purification of Tetrahymena. Many thanks are due to Mr. Mingjian Liu and Ms. Yalan Sheng, Institute of Evolution & Marine Biodiversity, OUC, for generously providing photos of Tetrahymena thermophila. This work was supported by the Natural Science Foundation of China (31522051, 31470064), the funding awarded to Weibo Song (15-12-1-1-jch), and the Qingdao National Laboratory for Marine Science and Technology, China. Yifan Liu was supported by National Sanitation Foundation (MCB 1411565), National Institute of Health (R01 GM087343), and the Department of Pathology at the University of Michigan.*

Barski, A., Cuddapah, S., Cui, K., Roh, T.Y., Schones, D.E., Wang, Z., Wei, G., Chepelev, I., and Zhao, K. (2007). High-resolution profiling of histone methylations in the human genome. Cell 129, 823–837.

Beh, L.Y., Muller, M.M., Muir, T.W., Kaplan, N., and Landweber, L.F. (2015). DNA-guided establishment of nucleosome patterns within coding regions of a eukaryotic genome. Genome Res 25, 1727–1738.

Brogaard, K.R., Xi, L., Wang, J.P., and Widom, J. (2012a). A map of nucleosome positions in yeast at base-pair resolution. Nature 486, 496–501.

Brogaard, K.R., Xi, L., Wang, J.P., and Widom, J. (2012b). A chemical approach to mapping nucleosomes at base pair resolution in yeast. In Method Enzymol, C. Wu, and C.D. Allis, eds. (Pasadena: California Institute of Technology), pp. 315–334.

Cassidy-Hanley, D., Bowen, J., Lee, J.H., Cole, E., VerPlank, L.A., Gaertig, J., Gorovsky, M.A., and Bruns, P.J. (1997). Germline and somatic transformation of mating *Tetrahymena thermophila* by particle bombardment. Genetics 146, 135–147.

Chalker, D.L., Meyer, E., and Mochizuki, K. (2013). Epigenetics of ciliates. CSH Perspect Biol 5, a017764.

Chen, X., Zhao, X., Liu, X., Warren, A., Zhao, F., and Miao, M. (2015). Phylogenomics of non-model ciliates based on transcriptomic analyses. Protein Cell 6, 373–385.

Cuatrecasas, P., Fuchs, S., and Anfinsen, C.B. (1967). Catalytic properties and specificity of the extracellular nuclease of *Staphylococcus aureus*. J Biol Chem 242, 1541–1547.

Cui, K., and Zhao, K. (2012). Genome-wide approaches to determining nucleosome occupancy in metazoans using MNase-Seq. In Chromatin Remodeling, R.H. Morse, ed. (Albany: Humana Press), pp. 413–419.

Eisen, J.A., Coyne, R.S., Wu, M., Wu, D., Thiagarajan, M., Wortman, J.R., Badger, J.H., Ren, Q., Amedeo, P., and Jones, K.M. (2007). Macronuclear genome sequence of the ciliate *Tetrahymena thermophila*, a model eukaryote. PLoS Biol 4, e286–e286.

Felsenfeld, G., and Groudine, M. (2003). Controlling the double helix. Nature 421, 448–453.

Flaus, A., Luger, K., Tan, S., and Richmond, T.J. (1996). Mapping nucleosome position at single base-pair resolution by using site-directed hydroxyl radicals. Proc Natl Acad Sci USA 93, 1370–1375.

Fraser, R.M., Keszenman-Pereyra, D., Simmen, M.W., and Allan, J. (2009). High-resolution mapping of sequence-directed nucleosome positioning on genomic DNA. J Mol Biol 390, 292–305.

Gao, F., Warren, A., Zhang, Q., Gong, J., Miao, M., Sun, P., Xu, D., Huang, J., Yi, Z., and Song, W. (2016). The all-data-based evolutionary hypothesis of ciliated protists with a revised classification of the phylum Ciliophora (Eukaryota, Alveolata). Sci Rep 6, 24874.

Gao, S., and Liu, Y. (2012). Intercepting noncoding messages between germline and soma. Genes Dev 26, 1774–1779.

Gao, S., Xiong, J., Zhang, C., Berquist, B.R., Yang, R., Zhao, M., Molascon, A.J., Kwiatkowski, S.Y., Yuan, D., and Qin, Z. (2013). Impaired replication elongation in *Tetrahymena* mutants deficient in histone H3 Lys 27 monomethylation. Genes Dev 27, 1662–1679.

Gorovsky, M., Glover, C., Johmann, C., Keevert, J., Mathis, D., and Samuelson, M. (1978). Histones and chromatin structure in *Tetrahymena* macro- and micronuclei. Paper presented at: Cold Spring Harb Sym (Woodbury: Cold Spring Harbor Laboratory Press).

Gorovsky, M.A. (1970). Studies on nuclear structure and function in *Tetrahymena pyriformis* II. Isolation of macro- and micronuclei. J Cell Biol 47, 619–630.

Gorovsky, M.A., Yao, M.C., Keevert, J.B., and Pleger, G.L. (1975). Isolation of micro- and macronuclei of *Tetrahymena pyriformis*. In Methods Cell Biol, D.M. Prescott, ed. (New York: Academic Press), pp. 311–327.

Greider, C.W., and Blackburn, E.H. (1985). Identification of a specific telomere terminal transferase activity in *Tetrahymena* extracts. Cell 43, 405–413.

Kaplan, N., Moore, I.K., Fondufe-Mittendorf, Y., Gossett, A.J., Tillo, D., Field, Y., LeProust, E.M., Hughes, T.R., Lieb, J.D., and Widom, J. (2009). The DNA-encoded nucleosome organization of a eukaryotic genome. Nature 458, 362–366.

Karrer, K.M. (1999). *Tetrahymena* genetics: two nuclei are better than one. In *Tetrahymena thermophila* (New York: Academic Press), pp. 127–186.

Karrer, K.M. (2012). Nuclear dualism. In *Tetrahymena thermophilia*, K. Collins, ed. (Waltham: Academic Press), pp. 29–52.

Kornberg, R.D. (1974). Chromatin structure: a repeating unit of histones and DNA. Science 184, 868–871.

Langmead, B., and Salzberg, S.L. (2012). Fast gapped-read alignment with Bowtie 2. Nat methods 9, 357–359.

Liu, J., Haorah, J., and Xiong, H. (2014). Western blotting technique in biomedical research. In Current laboratory methods in neuroscience research, H. Xiong, and H.E. Gendelman, eds. (New York: Springer), pp. 187–200.

Liu, Y., Mochizuki, K., and Gorovsky, M.A. (2004). Histone H3 lysine 9 methylation is required for DNA elimination in developing macronuclei in *Tetrahymena*. Proc Natl Acad Sci USA 101, 1679–1684.

Mavrich, T.N., Jiang, C., Ioshikhes, I.P., Li, X., Venters, B.J., Zanton, S.J., Tomsho, L.P., Qi, J., Glaser, R.L., and Schuster, S.C. (2008). Nucleosome organization in the *Drosophila* genome. Nature 453, 358–362.

Mochizuki, K., and Gorovsky, M.A. (2004). Small RNAs in genome rearrangement in *Tetrahymena*. Curr Opin Genet Dev 14, 181–187.

Moyle-Heyrman, G., Zaichuk, T., Xi, L., Zhang, Q., Uhlenbeck, O.C., Holmgren, R., Widom, J., and Wang, J.P. (2013). Chemical map of *Schizosaccharomyces pombe* reveals species-specific features in nucleosome positioning. Proc Natl Acad Sci USA 110, 20158–20163.

Nelson, J.D., Denisenko, O., and Bomsztyk, K. (2006). Protocol for the fast chromatin immunoprecipitation (ChIP) method. Nat Protoc 1, 179–185.

Ning, Y., Dang, H., Liu, G., Xiong, J., Yuan, D., Feng, L., and Miao, W. (2015). ATP-binding cassette transporter enhances tolerance to DDT in *Tetrahymena*. Sci China Life Sci 58, 297–304.

Noll, M., and Kornberg, R.D. (1977). Action of micrococcal nuclease on chromatin and the location of histone H1. J Mol Biol 109, 393–404.

O'Neill, L.P., and Turner, B.M. (2003). Immunoprecipitation of native chromatin: NChIP. Methods 31, 76–82.

Ozsolak, F., Song, J.S., Liu, X.S., and Fisher, D.E. (2007). High-throughput mapping of the chromatin structure of human promoters. Nat Biotechnol 25, 244–248.

Papazyan, R., Voronina, E., Chapman, J.R., Luperchio, T.R., Gilbert, T.M., Meier, E., Mackintosh, S.G., Shabanowitz, J., Tackett, A.J., Reddy, K.L., Coyne, R.S., Hunt, D.F., Liu, Y., and Taverna, S.D. (2014). Methylation of histone H3K23 blocks DNA damage in pericentric heterochromatin during meiosis. eLife 3, e02996.

Richmond, T.J., and Davey, C.A. (2003). The structure of DNA in the nucleosome core. Nature 423, 145–150.

Sahasrabuddhe, C.G., and Van Holde, K. (1974). The effect of trypsin on nuclease-resistant chromatin fragments. J Biol Chem 249, 152–156.

Schoeberl, U.E., and Mochizuki, K. (2011). Keeping the soma free of transposons: programmed DNA elimination in ciliates. J Biol Chem 286, 37045–37052.

Schones, D.E., Cui, K., Cuddapah, S., Roh, T.Y., Barski, A., Wang, Z.,

Wei, G., and Zhao, K. (2008). Dynamic regulation of nucleosome positioning in the human genome. Cell 132, 887–898.
Sims, R.J., Mandal, S.S., and Reinberg, D. (2004). Recent highlights of RNA-polymerase-II-mediated transcription. Curr Opin Cell Biol 16, 263–271.
Spadafora, C., Bellard, M., Lee Compton, J., and Chambon, P. (1976). The DNA repeat lengths in chromatins from sea urchin sperm and gastrula cells are markedly different. Febs Lett 69, 281–285.
Stein, L.D. (2013). Using GBrowse 2.0 to visualize and share next-generation sequence data. Brief Bioinform 14, 162–171.
Stover, N.A., Punia, R.S., Bowen, M.S., Dolins, S.B., and Clark, T.G. (2012). *Tetrahymena* Genome Database Wiki: a community-maintained model organism database. Database 2012, bas007.
Sweet, M.T., and Allis, C.D. (2005). Isolation and purification of *Tetrahymena* nuclei. CSH Protoc 2006, 878–878.
Thiriet, C., and Hayes, J.J. (2005). Chromatin in need of a fix: phosphorylation of H2AX connects chromatin to DNA repair. Mol Cell 18, 617–622.
Valouev, A., Ichikawa, J., Tonthat, T., Stuart, J., Ranade, S., Peckham, H., Zeng, K., Malek, J.A., Costa, G., and McKernan, K. (2008). A high-resolution, nucleosome position map of *C. elegans* reveals a lack of universal sequence-dictated positioning. Genome Res 18, 1051–1063.
Valouev, A., Johnson, S.M., Boyd, S.D., Smith, C.L., Fire, A.Z., and Sidow, A. (2011). Determinants of nucleosome organization in primary human cells. Nature 474, 516–520.
Verduyn, C., Van Kleef, R., Frank, J., Schreuder, H., Van Dijken, J., and Scheffers, W. (1985). Properties of the NAD(P)H-dependent xylose reductase from the xylose-fermenting yeast *Pichia stipitis*. Biochem J 226, 669–677.
Zentner, G.E., and Henikoff, S. (2013). Regulation of nucleosome dynamics by histone modifications. Nat Struct Mol Biol 20, 259–266.

SUPPORTING INFORMATION

Table S1 Number of purified MAC/MIC in each pellet ($\times 10^7$ per 1×10^8 cells)

Table S2 Light absorption values A_{260} of each fraction in UV compatible 96-well plates

The supporting information is available online at life.scichina.com and link.springer.com. The supporting materials are published as submitted, without typesetting or editing. The responsibility for scientific accuracy and content remains entirely with the authors.